Preparation and optical properties of Zr–Ce–O–N materials

S. Gutzov [a], M. Lerch [b],*

[a]St Kliment Ohridski University of Sofia, Department Physical Chemistry, 1. J. Bourchier Blvd, 1126 Sofia, Bulgaria
[b]University of Würzburg, Lehrstuhl Silicatchemie, Röntgenring 11, 97070 Würzburg, Germany

Abstract

Zr–Ce–O–N ceramics containing up to 10 cation% Ce and 15 anion% N have been prepared by the nitridation of Zr–Ce–O pellets at 1600–1900°C and P_{N_2} pressures between 1.4 and 1.6 bar. The phase relationships of the prepared materials are investigated using XRD. UV/V is reflectance spectra analysis shows that nitrogen incorporation changes the optical properties of Zr–Ce–O ceramics causing a brown–red coloration whose intensity depends on the nitrogen amount. © 2001 Elsevier Science Ltd. All rights reserved.

Keywords: Colour; Optical properties; Phase equilibria; Zr–Ce–O–N; $(Zr,Ce)O_2$

1. Introduction

In the last years a new class of ceramic materials — nitrogen-containing zirconia — have been obtained via direct nitridation of ZrO_2 at high temperatures in nitrogen atmosphere.[1–3] The chemical composition of quaternary nitrogen containing zirconia materials prepared in this way can be described as Zr–M–O–N where M = Ca, Mg, Y or Eu. The interest in the exploration of Zr–M–O–N ceramics was initially concentrated on the phase relationships based on oxygen vacancy formation. Anion vacancy formation in the zirconia lattice is the reason for the stabilization of normally metastable phases like cubic (c) or tetragonal (t).[4,5]

Not only phase formation and ionic conductivity[6] are of interest in nitrogen containing zirconia materials. Recently we found that nitrogen incorporation affects the optical properties of Zr–M–O–N if M is an optically active ion such as Eu(III).[7,8] We also observed that the optical properties of Zr–Eu(III)–O–N phases depend on the existence of oxygen vacancies and incorporated nitrogen ions, different chemical and/or coordinated activator sites and surface phenomena. These results show the value of a thorough study of the optical properties of nitrogen containing zirconia materials.

The aim of the present contribution is to study the phase relationships and optical properties of Zr–Ce–O–N materials. Cerium doped ceramics and powders are widely used as optical materials and as catalyst supports.[9–11]

2. Experimental methods

CeO_2 (Alpha, 99.9%) (1, 2.5, 5, 7.5, 10 mol%) was added to ZrO_2 powder (Alpha, 99 +). After grinding in a mortar the powder was pressed isostatically to pellets and sintered in air at 1600°C for 72 h. These pellets were nitrided for 2–4 h in a graphite heated resistance furnace (P_{N_2} = 1.4–1.6 bar) at temperatures of 1600, 1750 and 1900°C, respectively.

Qualitative and quantitative phase analysis using X-ray powder methods was carried out with a STOE STADIP diffractometer (Cu $K_{\alpha 1}$ radiation). For quantitative phase analysis we used the polymorph method described by Garvie and Nicolson and the VISUAL X^{POW} software.[12,13] Room temperature UV/Vis reflectance spectra from 300 to 800 nm were obtained with a Shimadzu MPC-3100 spectrometer using a 1 mm special glass cell (transmittance 80–90% between 320 amd 1500 nm) and $BaSO_4$ as reference material for all measurements. From the measured reflectance in % we calculated the relative absorbance A_{KM} with the Kubelka–Munk function.[14]

* Corresponding author.
E-mail address: lerch@fks.chem.tu-berlin.de (M. Lerch).

An attempt was made to excite the Zr–Ce–O–N sample luminescence on a Perkin–Elmer LS50B spectrometer with a monochromator slit of 2.5–10 nm and excitation wavelengths between 220 and 500 nm.

N/O analysis of the samples were performed using the method of hot gas extraction (LECO).

3. Experimental results and discussion

3.1. Phase relationships and defect chemistry

Table 1 depicts the qualitative and quantitative phase composition of the samples investigated, the percentage of CeO_2 added, the experimentally determined amount of nitrogen and the chemical formula calculated. Representative XRD diagrams from the samples investigated are shown in Fig. 1.

In Table 1 the presence of the following crystalline phases is indicated:

1. The well known zirconia phases such as cubic (c), tetragonal (t) and monoclinic zirconia (m). In non-nitrided samples the monoclinic phase is dominating. This finding correlates with the ZrO_2–CeO_2 phase diagram.[15] In nitrided samples, hovever, the content of the stabilized phases increases.
2. In samples ce11750 and ce11900 we detected the existence of the so called β''^3 structure type. Recently,[5] we have shown that the β'' structure formation is connected with the ordering kinetics

on cooling cubic or tetragonal high temperature phases.
3. In some of the samples small amounts of cubic ZrN (JCPDC 31-1493) have been observed.
4. Sample ce101600 shows additional reflections which belong to a new as yet unknown crystalline phase. This seems to be similar to a phase known from the Zr–Eu–O–N system, $Zr_{0.53}Eu_{0.46}O_{1.68}N_{0.06}$.[8]

Fig. 2 depicts the amount of monoclinic phase (Xm) as a function of the Ce content for different nitridation conditions. For non-nitrided samples, Xm does not depend on the Ce content. Thus, in the process of the ZrO_2–CeO_2 air heating the oxidation number of Ce remains IV as in CeO_2.

In all nitrided samples the value of Xm dramatically falls as a result of nitrogen incorporation into the zirconia lattice. This process is accompanied by oxygen vacancy formation as expressed in the following Eq:[1–3]

$$N_2(g) + 3O_O^x = 2N_O' + V_O^{oo} + 1.5O_2(g) \qquad (1)$$
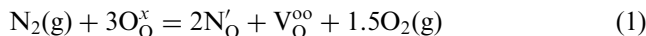
According to this equation the charge balance following nitrogen incorporation is

$$[V_O^{oo}] = 2[N_O'] \qquad (2)$$

where $[N_O']$ represents the site fraction of nitrogen in zirconia given by the N-analysis (Table 1). A comparison with the Xm values given in Table 1 shows that

Table 1
Nitrogen amount (N), monoclinic phase percent (Xm), results of the phase analysis, calculated formula and preparation temperature (T_p) of the prepared samples (the notation of the nitrided samples also gives the nitridation temperature; for nitrogen-containing samples, T_p is the nitridation temperature)

Samples	N (%)	Xm (%)	Phases[a]	Calculated formula	T_p (°C)
ce1	0	100	m	$Zr_{0.99}Ce_{0.01}O_2$	1600
ce11600	0.165	96	m,t	$Zr_{0.99}Ce_{0.01}O_{1.98}N_{0.015}$	1600
ce11750	1.948	43	m,t, β''	$Zr_{0.99}Ce_{0.01}O_{1.75}N_{0.17}$	1750
ce11900	1.859	51	m,t, β''	$Zr_{0.99}Ce_{0.01}O_{1.76}N_{0.16}$	1900
ce25	0	100	m	$Zr_{0.98}Ce_{0.02}O_2$	1600
ce251600	0.363	97	m,t	$Zr_{0.98}Ce_{0.02}O_{1.95}N_{0.032}$	1600
ce251750	2.162	7	c,m,<u>t</u>	$Zr_{0.98}Ce_{0.02}O_{1.72}N_{0.18}$	1750
ce251900	1.771	12	c,m,<u>t</u>	$Zr_{0.98}Ce_{0.02}O_{1.77}N_{0.08}$	1900
ce5	0	98	m,t	$Zr_{0.95}Ce_{0.05}O_2$	1600
ce51600	0.482	29	c,m,t	$Zr_{0.95}Ce_{0.05}O_{1.94}N_{0.04}$	1600
ce51750	2.315	0	c,ZrN	$Zr_{0.95}Ce_{0.05}O_{1.70}N_{0.20}$	1750
ce51900	3.277	0	c,ZrN	$Zr_{0.95}Ce_{0.05}O_{1.57}N_{0.28}$	1900
ce75	0	100	m	$Zr_{0.93}Ce_{0.07}O_2$	1600
ce751600	0.797	0	c	$Zr_{0.93}Ce_{0.07}O_{1.90}N_{0.07}$	1600
ce751750	2.046	0	c,ZrN	$Zr_{0.93}Ce_{0.07}O_{1.73}N_{0.18}$	1750
ce751900	3.107	0	c,ZrN	$Zr_{0.93}Ce_{0.07}O_{1.60}N_{0.14}$	1900
ce10	0	96	m,t/c	$Zr_{0.9}Ce_{0.1}O_2$	1600
ce101600	0.115	89	m,c,?	$Zr_{0.9}Ce_{0.1}O_{1.98}N_{0.01}$	1600
ce101750	1.621	0	c	$Zr_{0.9}Ce_{0.1}O_{1.79}N_{0.14}$	1750
ce101900	1.754	0	c	$Zr_{0.9}Ce_{0.1}O_{1.77}N_{0.15}$	1900

[a] Phases: m — monoclinic, t — tetragonal, c — cubic zirconia, β''-$Zr_7O_{9.2}N_{3.2}$, ? — new phase.
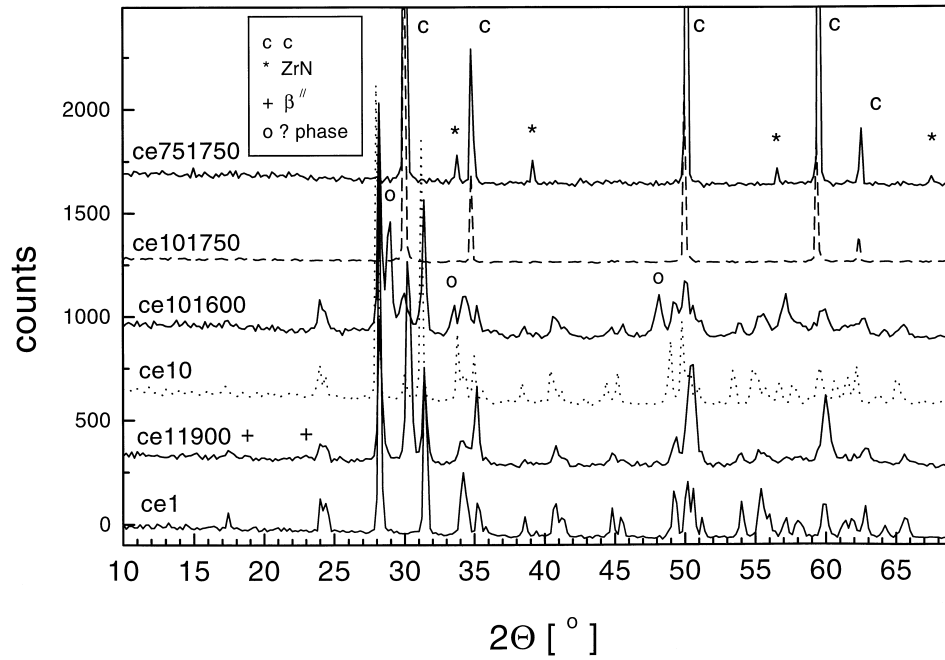
Fig. 1. XRD-diagrams of Zr–Ce–O–N powders. The phase abbreviations are the same as is Table 1. The non-marked reflections belong to monoclinic (m) zirconia.
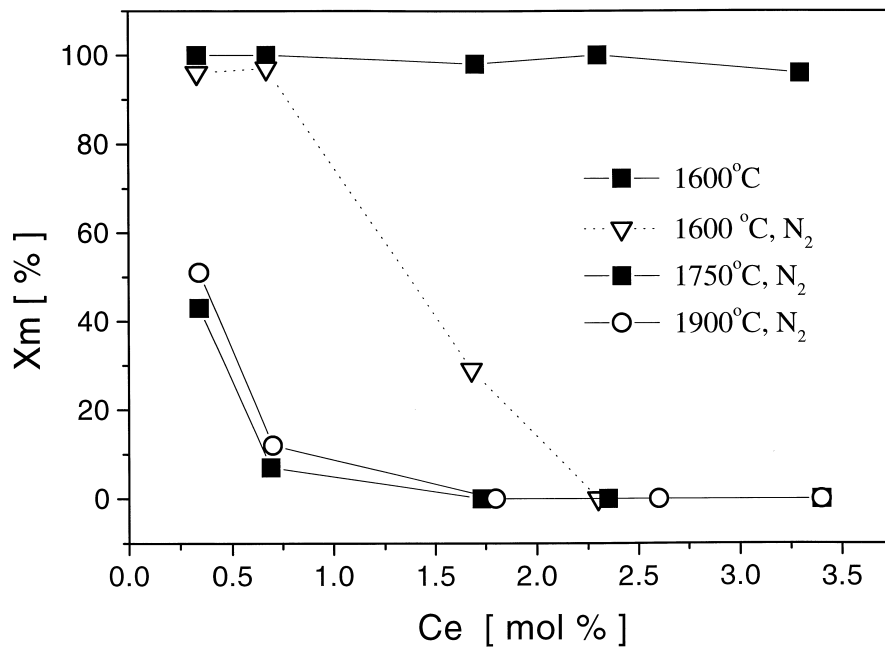

Fig. 2. Monoclinic zirconia percent Xm vs Ce amount at different nitridation conditions.

Xm = 0 at $[N_O']$ greater than 5–6%. In this way we can conclude that the stability of the stabilized zirconia phases depends on the oxygen vacancy concentration.

Fig. 3 presents the dependence of the N content on the amount of Ce in the investigated samples. In the case of the Zr–Ce–O–N system, the N vs Ce content dependencies reach a maximum at 2–3 anion site fraction %N.

For 1900°C where the system reaches equilibrium[4] we calculated the equilibrium constant K for the nitrogen incorporation described by Eq. (1). In the case that Ce has an oxidation number IV (see next section) we can write the following equation for K by using Eqs. (1). and (2):

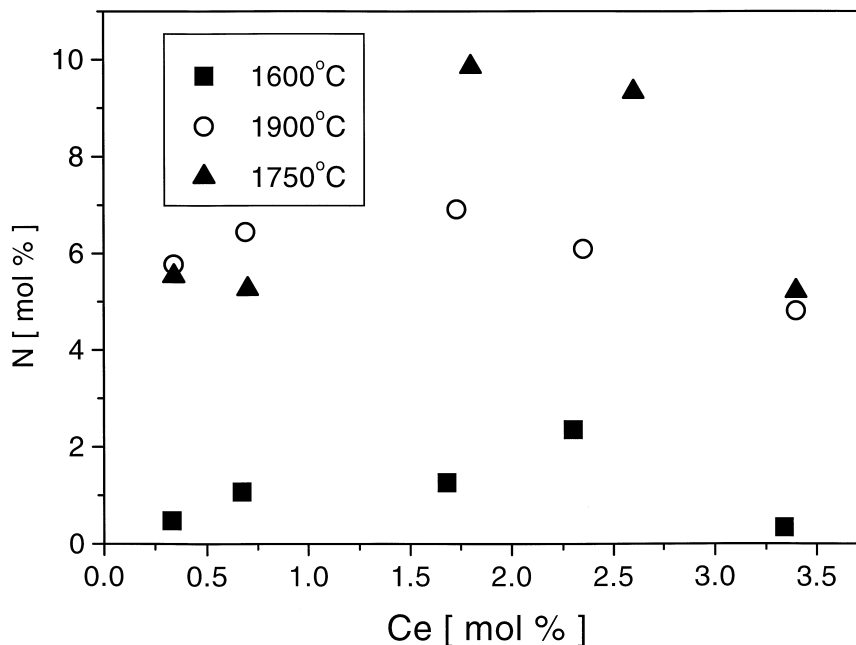$$K(P_{O_2})^{-3/2}P_{N_2} = \frac{(4[V_O^{oo}]^3)}{(1 - 3[V_O^{oo}])^3} \tag{3}$$

Fig. 3. Nitrogen vs Ce amount at different nitridation temperatures.

P_{O_2} is the oxygen pressure at 1900°C which can be calculated to 5×10^{-15} bar[4].

P_{N_2} is the nitrogen pressure at 1900°C, 1.6 bar.

K is calculated by linearization (R-factor 0.99) of Eq. (3) to be 1.1×10^{-24}, which is very similar to the values for Zr–Y–O–N (1×10^{-25}) or Zr–Eu–O–N (9.6×10^{-25}) materials.[5,8] The larger value of K in the Zr–Ce–O–N system, however, indicates that nitrogen incorporation may be facilitated by the absence of aliovalent dopants like Y(III) and Eu(III). A comparison with Zr–Ca–O–N and Zr–Mg–O–N materials gives K-values of 2×10^{-25} and 1×10^{-25},[4] respectively in agreement with this assumption.

3.2. Optical properties

None of the Zr–Ce–O–N samples showed luminescence at 220–500 nm excitation. For Ce(III) doped materials, a strong luminescence has to be expected.[9,10] The absence of luminescence indicates that most of the Ce(IV) ions do not change their valency in the nitridation process.

The nitridation dramatically changes the color of the Zr–Ce–O materials. As a result of the nitridation the Zr–Ce–O powders became brown–red depending on the nitridation conditions and N content. The coloration disappears after a short time of heating in air at 600°C.

There are earlier contributions reporting on the coloration of oxides at nitridation. In the system Zr–Eu–O–N, we described a pink coloration coming from a weak absorption transition at 530–550 nm in nitrogen containing materials reheated in air.[7,8] There are also data for coloration of Zr–Ta–O–N materials.[16] In our

former investigations we explained the coloration after nitridation with the existence of $N^{3-} \rightarrow Zr^{4+}$ or Eu^{3+} charge transfer transitions (CTT).[7,8] In this way the strong intensity of these absorption transitions could be explained. Another possibility for coloration may be the formation of color centers by nitridation. The red coloration of the Zr–Ce–O–N materials can be similarly explained, either as $N^{3-} \rightarrow Zr^{4+}$ or Ce^{4+} CTT or as color centers (electrons trapped in anion vacancies).

It would be interesting to describe quantitatively how the complicated surface processes which take place on nitridation can affect the optical properties of Zr–O–N materials.

In Fig. 4 typical UV/V is absorption spectra of Zr–Ce–O–N materials are shown. The relative absorbance A_{KM} is calculated from the measured reflectance spectra using the Kubelka–Munk[14] function.

An intensive broad absorption transition at 480 nm due to N-incorporation can be seen. The UV/Vis spectra of Ce(IV) and Ce(III) compounds are given for comparison. Ce(III) and Ce(IV) ions show a different behaviour and could not be responsible for the described absorption transition. The Zr–Ce–O materials are white, displaying a strong absorption transition in the UV region coming from $O^{2-} \rightarrow Zr^{4+}$, Ce^{4+} CTT.

We treated all Zr–Ce–O–N spectra mathematically as overlapped Gaussian peaks where the maximum of the first absorption peak is in the UV region (the $O^{2-} \rightarrow Zr^{4+}$, Ce^{4+} CTT) and the second one is in the visible region (the $N^{3-} \rightarrow Zr^{4+}$ or Ce^{4+} CTT). For all spectra we obtained good fitting results where the χ^2 factor was between 0.001 and 0.003. In this way we obtain the height, the spectral maxima and the half

width of every absorption peak. The half width of the 480 nm absorption transition is varying between 4500 and 7500 cm^{-1}. In Fig. 4, a Gaussian deconvolution of the Zr–Ce–O–N absorption spectra is shown.

The maximal relative absorbance A_{KM} in the region of the absorption peaks (the height of the absorption peaks) depends dramatically on the N content. In Fig. 5 the maximal relative absorption vs the nitrogen content for Zr–Ce–O–N materials is presented. At low N content,

the function is linear according to the Bouguer–Lambert–Beer law. At high N concentrations, the relative absorption decreases indicating the formation of different N optical centers or the maximal possible nitrogen concentration. Using the linear part of the curve, the amount of the "primary" N optical centers can be obtained by interpolation.

Fig. 6 presents the wavenumber of the N-dependent absorption transition from the measured N content.
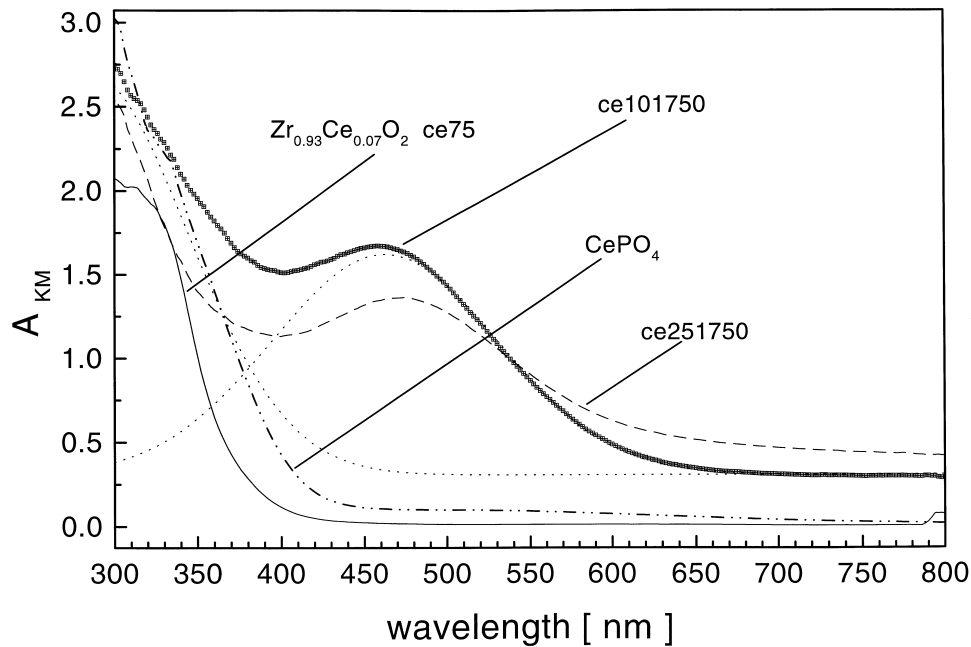

Fig. 4. UV/Vis absorption spectra of Zr–Ce–O–N (ce251750 and ce101750, Table 1) powders. The spectra of Ce(III) (CePO$_4$) and Ce(IV) (Zr$_{0.93}$Ce$_{0.07}$O$_2$) powders are given for comparison. A Gaussian deconvolution of the ce101750 spectrum is shown.
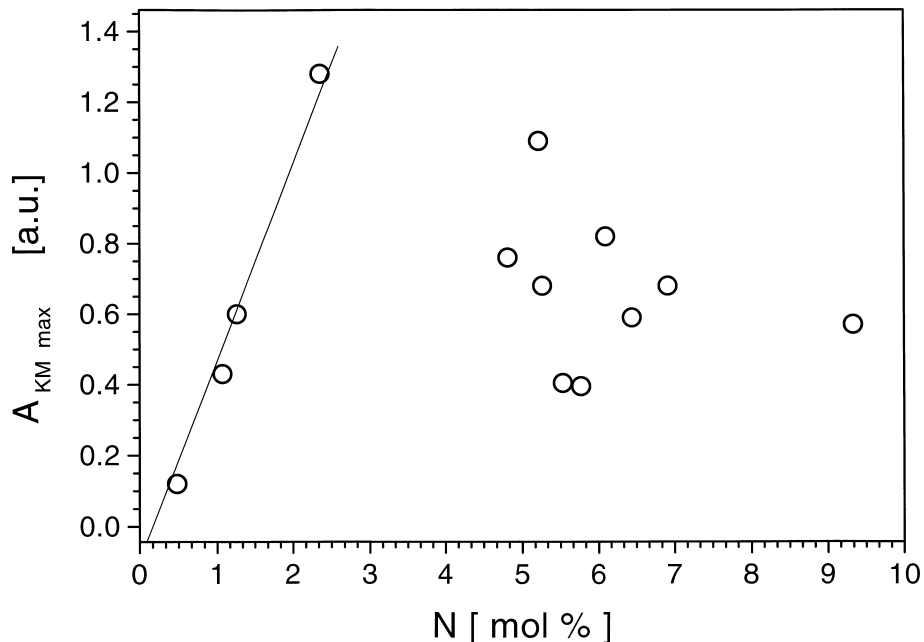

Fig. 5. Maximal relative absorbance vs nitrogen concentration dependence for Zr–Ce–O–N powders.

The increase of the energy of the transition indicates a decrease of the average N–Ce (Zr) distances in the zirconia crystal lattice with increasing N content. It is interesting to note, that the wavenumber of the transition in Fig. 6 between 20 200 and 21 600 cm^{-1} (495–463 nm) partially coincides with an optical absorption band in yttrium-stabilized tetragonal zirconia at 480 nm, caused by γ-irradiation.[17]

Fig. 7 depicts the dependence of the cubic zirconia lattice constant on the content of incorporated nitrogen.

A decrease of the lattice constant which may be a possible explanation for the increase of the energy of the nitrogen depending absorption transition is shown in Fig. 7.

The color of the Zr–Ce–O–N materials depends both on the maximal relative absorbance and absorption peak position as well as on the zirconia phase prepared. Only cubic samples with a nitrogen content of 2.5–5 mol% have a red color. Samples with an N amount less than 1.5 mol% are grey. The other samples are brown–red colored.
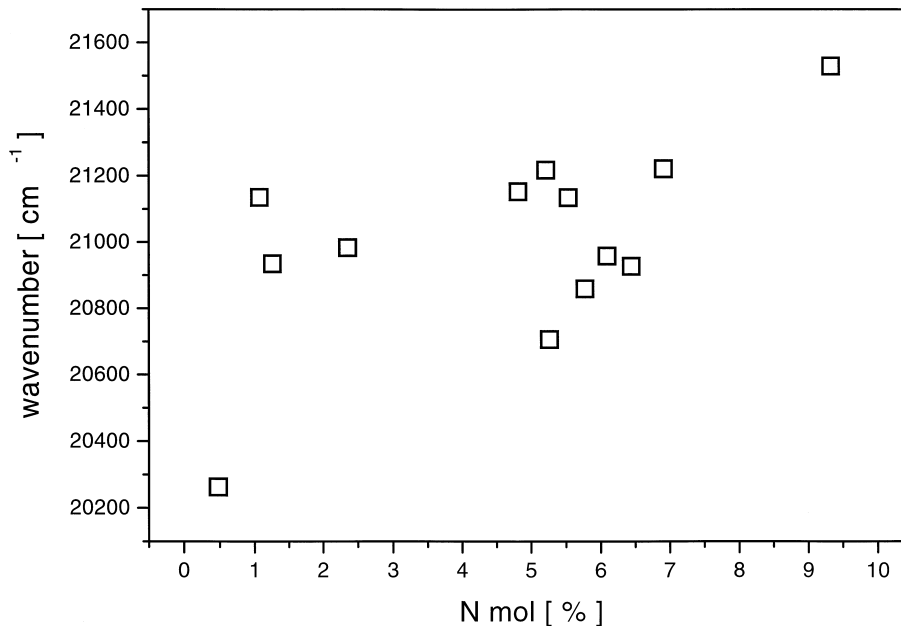

Fig. 6. Energy of the 480 nm absorption transition vs the nitrogen amount. The increase of the energy of the transition indicates an decrease of N–Ce (Zr) distances.
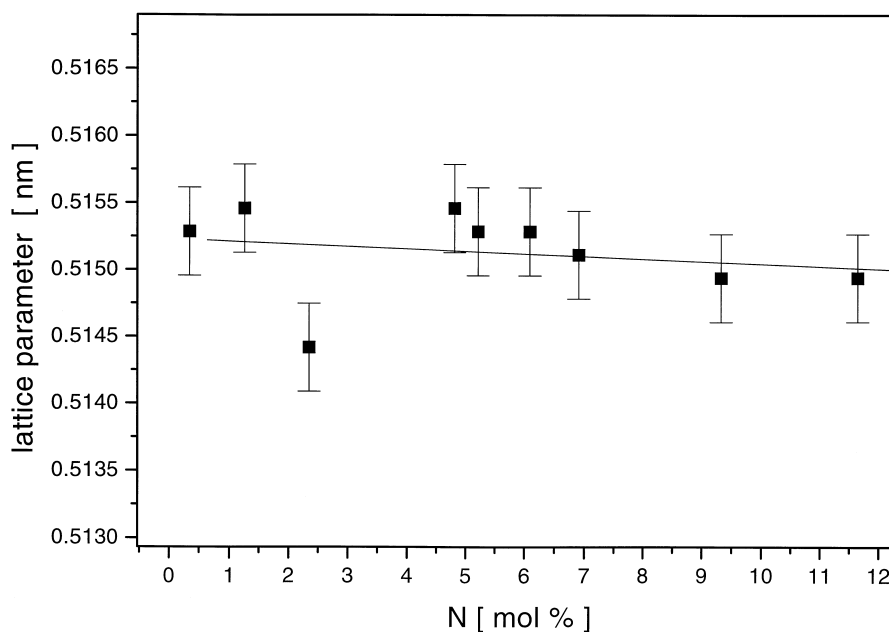

Fig. 7. Lattice parameter of the cubic Zr–Ce–O–N materials as function of the nitrogen amount.

4. Conclusions

We have investigated the phase relationships and optical properties of Zr–Ce–O–N materials. The stability of the stabilized zirconia phases depends on the oxygen vacancy formation due to nitrogen incorporation. It seems that under the conditions of direct nitridation the oxidation number of the cationic dopant in the zirconia lattice remain unchanged. The nitridation changes the optical properties of the zirconia ceramics reversibly by the presence of N^{3-} charge transfer transitions or color center formation.

Acknowledgements

References

1. Cheng, Y. B. and Thompson, D. P., Nitrogen-containing tetragonal zirconia. *J. Am. Ceram. Soc.*, 1991, **74**, 1135–1138.
2. Cheng, Y. B. and Thompson, D. P., Role of anion vacancies in nitrogen-stabilized zirconia. *Am. Ceram. Soc.*, 1993, **76**, 683–688.
3. Lerch, M., Nitridation of zirconia. *J. Am. Ceram. Soc.*, 1996, **79**, 2641–2644.
4. Lerch, M., Wrba, J. and Lerch, J., Vacancy ordering in the ZrO$_2$ rich part of the systems Ca–Zr–O–N, Mg–Zr–O–N, and Y–Zr–O–N. *J. Solid State Chem.*, 1996, **15**, 2127–2129.
5. Wrba, J. and Lerch, M., Phase relationships in the ZrO$_2$-rich part of the systems Y–Zr–N–O, Ca–Zr–N–O and Mg–Zr–N–O up to temperatures of 1150°C. *J. Eur. Ceram. Soc.*, 1998, **18**, 1787–1793.
6. Wendel, J., Lerch, M. and Laqua, W., Novel zirconia-based superionic conductors: the electrical conductivity of Y–Zr–O–N materials. *J. Solid State Chemistry*, 1999, **142**, 163–167.
7. Gutzov, S., Kohls, M. and Lerch, M., The luminescence of Zr–Eu–O–N materials. *J. Phys. Chem. Solids*, 2000, **61**, 1301–1309.
8. Gutzov, S., Lerch, J. and Lerch, M., submitted for publication.
9. Schlotter, P., Schmidt, R. and Schneider, J., Luminescence conversion of blue emitting diodes. *Appl. Phys. A*, 1997, **64**, 417–418.
10. El Jouhari, N., Parent, C. and Le Flem, G., Photoluminescence of Ce^{3+}, Tb^{3+} and Mn^{2+} in glasses of base composition LaMgB$_5$O$_1$. *J. Solid State Chemistry*, 1996, **123**, 398–407.
11. Martinez-Arias, A. and Soria, J. C., Spectroscopic study of active phase support interactions on a RhO$_x$/CeO$_2$ catalyst evidence for electronic interactions. *J. Catalysis*, 1997, **168**, 364–373.
12. Garvie, R. C. and Nicholson, P. S., Phase analysis in zirconia systems. *J. Am. Ceram. Soc.*, 1972, **55**, 303–305.
13. STOE, *VISUAL X^{POW}*, Version 2.67. Darmstadt, 1995.
14. Schmidt, W., *Optische Spektroskopie*. VCH, Weinheim, 1994, pp. 317–323.
15. Green, D. J., Hannink, R. H. J. and Swain, M. V., *Transformation Toughening of Ceramics*. CRC Press, Boca Raton, FL, 1989, pp. 1–30.
16. Rahäuser, O., *Synthese und Hochtemperaturverhalten von Nitriden und Nitridoxiden der Elemente Nb, Ta und W*. University of Würzburg, 1998.
17. Dietrich, A., Heimann, R. B. and Willmann, G., The colour of medical grade zirconia (Y-TZP). *J. Mater. Sci.: Mater. Med.*, 1996, **7**, 559–565.